Coordination Chemistry Reviews 253 (2009) 2036–2048

Contents lists available at ScienceDirect

Coordination Chemistry Reviews

journal homepage: www.elsevier.com/locate/ccr

Review

Aza-deficient porphyrin as a ligand

Ewa Pacholska-Dudziak, Lechosław Latos-Grażyński*

Department of Chemistry, University of Wrocław, ul. F. Joliot-Curie 14, 50-383 Wrocław, Poland

Contents

ARTICLE INFO

Article history:
Received 25 November 2008
Accepted 26 January 2009
Available online 5 February 2009

Keywords:
Porphyrinoids
Annulene
Aromaticity
Conformation analysis
Nickel
Palladium
Cadmium
Zinc
Möbius antiaromaticity

ABSTRACT

Vacataporphyrin, a porphyrin devoid of one nitrogen atom is an annulene–porphyrin hybrid. Naming it in a different manner—butadieneporphyrin as one pyrrole unit is replaced with butadiene moiety, accents its carbaporphyrinoid nature. The molecule acts as a macrocyclic ligand which accommodates the following metal ions: cadmium(II), zinc(II), nickel(II) and palladium(II). The tripyrrin pincer of vacataporphyrin holds the metal close to the flexible butadiene fragment which may acquire different configurations depending on presence of light, acid concentration or axial ligand identity. The butadiene moiety of vacataporphyrin may be involved in a π-interaction with metal ions. A single example a σ palladium(II)–carbon bond has also been identified. Intricate multi-step structural changes have been spectroscopically detected for palladium(II) vacataporphyrin. A peculiar reversible switch between vacataporphyrin conformers characterized by Hückel or Möbius topology has been accompanied by a change of electronic structure revealed respectively by aromaticity or antiaromaticity.

* Corresponding author.
E-mail address: LLG@wchuwr.pl (L. Latos-Grażyński).

0010-8545/$ – see front matter © 2009 Elsevier B.V. All rights reserved.
doi:10.1016/j.ccr.2009.01.029

1. Introduction

Vacataporphyrin (butadieneporphyrin) **1** [1], an aza-deficient porphyrin is a molecule located on an intersection of several lines of porphyrinoid research such as heteroporphyrins, vinylogous porphyrins, carbaporphyrins, triphyrins and expanded porphyrins. This brief overview is expected to facilitate an appreciation of the crossbreed nature of **1**, illustrating major features of listed porphyrinoids directly related to vacataporphyrin. In particular the representative examples of porphyrinoids which contain annulene-like fragments built into the macrocyclic structure have been gathered.

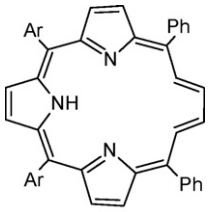

1

The skeleton. Initially one can notice, that the skeleton of vacataporphyrin may be readily colligated with that of texaphyrin **2** [2] or an expanded non-aromatic porphyrinoid **3** [3].

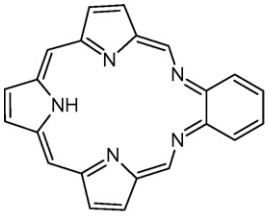

2

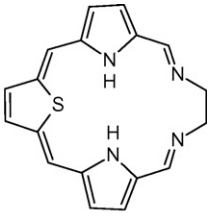

3

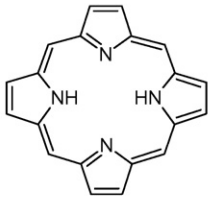

4

The size of texaphyrin coordination core with five nitrogen atoms exposed for coordination is evidently larger than that of a porphyrin (**4**). In vacataporphyrin the number of atoms in the inner perimeter remains the same as in **2**, 17, but obviously the coordination ability of CH groups is not comparable with that of nitrogen atoms. Texaphyrin is a suitable receptor for several transition and inner transition metal ions and typically uses five nitrogen atoms to bind a central metal ion although rare examples of coordination using three nitrogen donors have been documented as well [4,5]. The coordination chemistry of texaphyrin has been intensively explored considering their potential medical application. For instance the gadolinium(III) and lutetium(III) complexes were checked in advanced clinical trials as adjuvants for the radiation- and irradiation-based treatment of cancer and cardiovascular disease [6,7].

2. Annulene motif in porphyrin chemistry

2.1. Regular porphyrins

Much attention has been focused on the annulenic character of porphyrins, "bridged annulenes of nature" [8], in connection with their aromatic character (in the Hückel's definition sense) and construction of porphyrin isomers [9]. Porphyrin may be regarded as an diaza [18] annulene with two nitrogen and two ethylene bridges (**4b**). Some arguments point out different models to be of preference: a [20]annulene dication bridged with two neutral and two negatively charged nitrogen bridges (**4c**) or tetraaza[16]annulene dianion with dicarbon bridges (**4a**) [10,11].

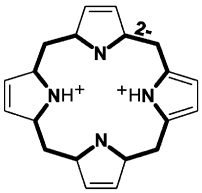

4a

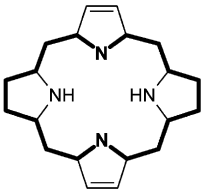

4b

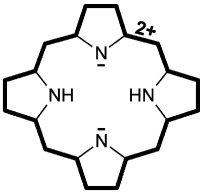

4c

2.2. Opened pyrrolic subunits; corrupted porphyrins

In search for a "most relevant conjugation pathway" of porphin, norporphines **5** and **6** (names proposed by Flitsch: isobacteriophin and bacteriophin respectively) were synthesized [12,13]. They are in fact parent compounds for many porphyrinoids of biological importance, like isobacteriochlorin and bacteriochlorin. The molecules **5**, **6** and **7** are derived from porphin. They are formally created by removal of one (**7**) or two (**5**, **6**) β-ethylene bridges, disassembling one or two pyrrole units. Actually a different way of a porphyrin "stripping down" (preserving 18- and 20-member conjugation pathways) gives the title vacataporphyrin **1**.

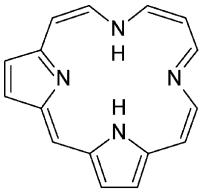

5

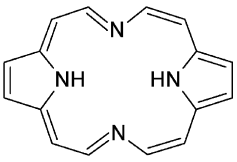

6

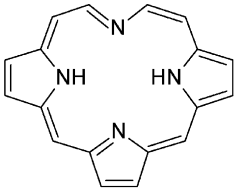

7

The third member of the norporphyrin family, **7** (chlorophin) was synthesized in its substituted form in oxidative ring-opening of an (octadehydrocorrinato)nickel(II) salt in course of investigations on green hemes [14]. In independent studies concerning a catabolism of chlorophyll a related porphyrinoid was detected. Thus in a two-step oxidation reaction of nickel porphyrin complex, dihydroxylation and then cleavage of β–β bond took place

and yielded aromatic 2,3-secochlorin-2,3-dione nickel complex for both, octaethyl and tetraphenyl (**8**) derivatives [15,16].

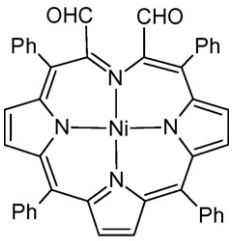

8

2.3. Porphyrin vinylogs

In analogy to larger annulenes, vinylogously enlarged porphyrins, exemplified here by [30]porphyrin(1.7.1.7) **9** [17], and their heteroanalogues were designated. Such molecules, which break records of the diatropic ring current, were advertized as "superarenes" [18]. They constitute a branch of expanded porphyrins, placed between rigid porphyrins and conformationally unstable non-bridged annulenes [19–24].

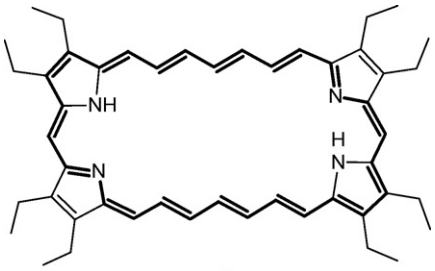

9

Large macrocylic systems like tetraepoxy[32]annulenes (6.2.6.2), **10**, synthesized by Märkl et al., exist as mixtures of several antiaromatic conformers two of which have been isolated, (*Z*,*E*,*E*,*E*,*Z*,*E*,*E*,*E*) **10a** and (*E*,*Z*,*E*,*E*,*E*,*Z*,*E*,*E*) **10b** (the diastereoisomers are identified by the configurations of *meso* linkers) [24]. The annulenes **10** are highly flexible because the (*E*)-ethenediyl bridges rotate around the adjacent σ-bonds. Oxidation of [32]annulenes(6.2.6.2) **10a** and **10b**, gives a mixture of four stereoisomeric tetraoxa[30]porphyrin(6.2.6.2) dications, **11a**/**11a′**/**11b**/**11c**. Their ^{1}H NMR $\Delta\delta$ (δ_{out}–δ_{in}) values (26.81, 25.83, 27.25 and 21.11 ppm respectively) indicate the aromatic character of the dications **11**, accepting a diatropic ring current effect as the aromaticity criterion.

2.4. Heteroporphyrins and carbaporphyrinoids

21-Vacataporphyrin **1** is also directly related to 21-heteroporphyrins with a general formula **12**, presuming that instead of a heteroatomic bridge a vacant space is incorporated.

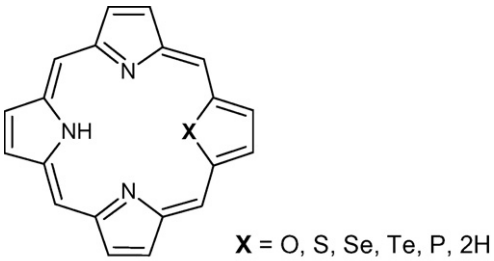

12

In fact the valence of each α-carbon of the cleaved heterocyclic ring is completed by a hydrogen atom, and the C–H bonds are directed inward the coordination core. Therefore formally, the heteroatom **X** substitution for hydrogen atoms gives the 21-vacataporphyrin. Heteroporphyrinoids are peculiar macrocyclic ligands which preserve the basic features of porphyrin skeleton with a specific donor heteroatom favorably oriented toward a coordinated transition metal ion. These porphyrinoids offered a new strategy for stabilization of rare cases of furan, phosphole, thiophene or selenophene η^1-coordination [25–28]. 21-Vacataporphyrin preserves some coordination properties of 21-heteroporphyrins except that in this case instead of 21-heteroatom the non-bridged annulenic fragment is held in proximity of a metal ion.

Carbaporphyrins may be considered as exceptional representatives of heteroporphyrins, with carbon paradoxically nominated as heteroatom. Carbaporphyrin chemistry exploded in recent years with several exciting new molecules, like inverted porphyrins, a family of benziporphyrins, azuliporphyrins, benzocarbaporphyrins which all serve as ligands for transition metal ions [26,29–33]. The unique organometallic chemistry is developed in the restricted geometry of coordination core imposed by carbaporphyrinoids. Such a peculiar environment allows one to address several fundamental questions of interactions which involve the metal ion-(C_{core}–H) fragment. Actually a whole spectrum of situations including such extremes as a covalent metal–carbon bond (**13**) or π weak interactions (**14**) has been covered [26,29,30,34]. The fine switching of a coordination geometry from trigonal to tetrahedral applying the perimeter modification has been of peculiar interest [35].

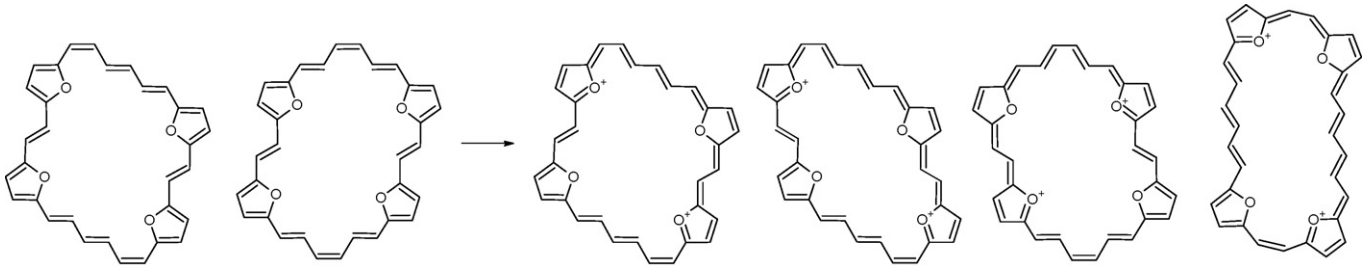

10a **10b** **11a** **11a'** **11b** **11c**

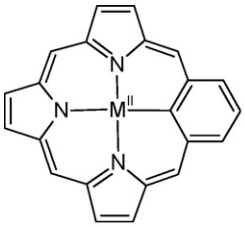

13

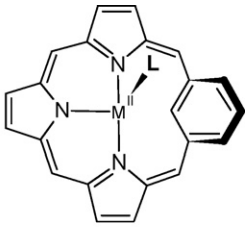

14

The *para*-benziporphyrin structure **15** [36] brings a significant analogy relevant to understanding of vacataporphyrin **1** properties. Formally two limiting conformations of vacataporphyrin, $\mathbf{1_A}$ and $\mathbf{1_B}$, are imprinted into the *p*-benziporphyrin frame. The π delocalization of **15** involves alternatively an inner or outer phenylene perimeter. Thus drawing a parallel to carbaporphyrinoids, in order to make a point about the nature of the pyrrole replacing moiety, the name "butadieneporphyrin" seems to be more appropriate to account for flexibility and coordination properties of **1**.

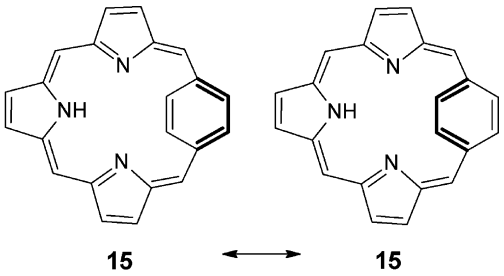

15 ⟷ **15**

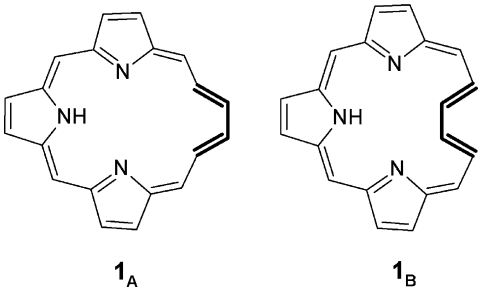

$\mathbf{1_A}$ $\mathbf{1_B}$

15 is flexible because of the mobile *p*-phenylene ring. A seesaw motion of this moiety is fast on the ^{1}H NMR scale and gives rise to averaging of the inner and outer protons chemical shifts at 295 K. The molecule is diatropic, contrary to *meta*-benziporphyrin, where the macrocyclic aromaticity is absent as a consequence of incompatibility between the porphyrinoid and benzenoid delocalization modes [37]. In fact the structural motif of –CH=CH– fragment directed into the porphyrin cavity was originally discovered for 21,23-ditelluraporphyrin **16** [38].

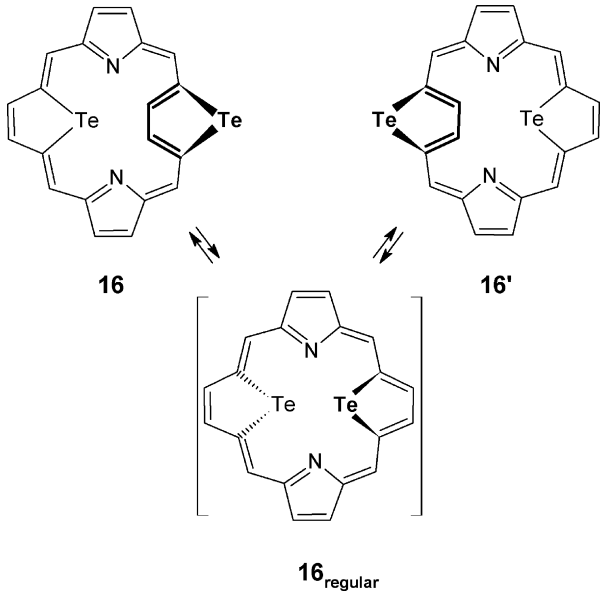

16 ⇌ **16'**

$\mathbf{16}_{\text{regular}}$

Presumably the size of the tellurium atoms is instrumental in the remarkable distortion of macrocycle **16**. One of the tellurophene moieties is coplanar with two pyrrole rings while the second is flipped and its tellurium atom is directed away from the center of the macrocycle. The remarkable flipped structure **16** detected in the solid state is preserved in solution, as determined by ^{1}H NMR studies. The inner and outer β-H tellurophene resonances are easily distinguishable due to a small, but still present aromatic ring current effect, with $\Delta\delta$ equal only 2.45 ppm. The molecule **16** in solution interchanges between two energetically and structurally identical flipped forms **16** and **16′** with a meaningful contribution of a regular conformation $\mathbf{16}_{\text{regular}}$.

In a tetrapyrrolic framework such ring inversion has been observed for N-confused porphyrin. The flipping of the N-confused pyrrolic moiety may be trapped by iridium(I) coordination [39], dimer formation [40] or leads to fused porphyrin **17** [41].

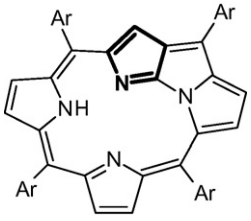

17

2.5. Triphyrins

The alternative name of vacataporphyrin, [18]triphyrin(6.1.1), places the molecule in the subclass of contracted porphyrins described by a general formula [*n*]triphyrin(*n*.1.1) (*n* = 1, 2, . . .). The porphyrin ring modification by eliminating one pyrrole/heterocyclic ring has driven some attention. Triphyrins exemplified by ethyneporphyrins **18**, **19** [42,43], *meso*-ethynyl triphyrin(1.1.3) **20** [44], subpyriporphyrin **21** [45], triphyrin(2.2.2) **22**

[46,47] or basic [14] triphyrin(1.1.1) called subporphyrins, trapped as boron complexes **23** [48], azatriphyrin(1.1.4) **24** with one furan ring [3,49] have shrunk coordination cores. Vacataporphyrin, although a triphyrin, is paradoxically an expanded porphyrin, considering Sessler's definition of an expanded porphyrin as a porphyrinoid with 17 atoms in the inner perimeter [4].

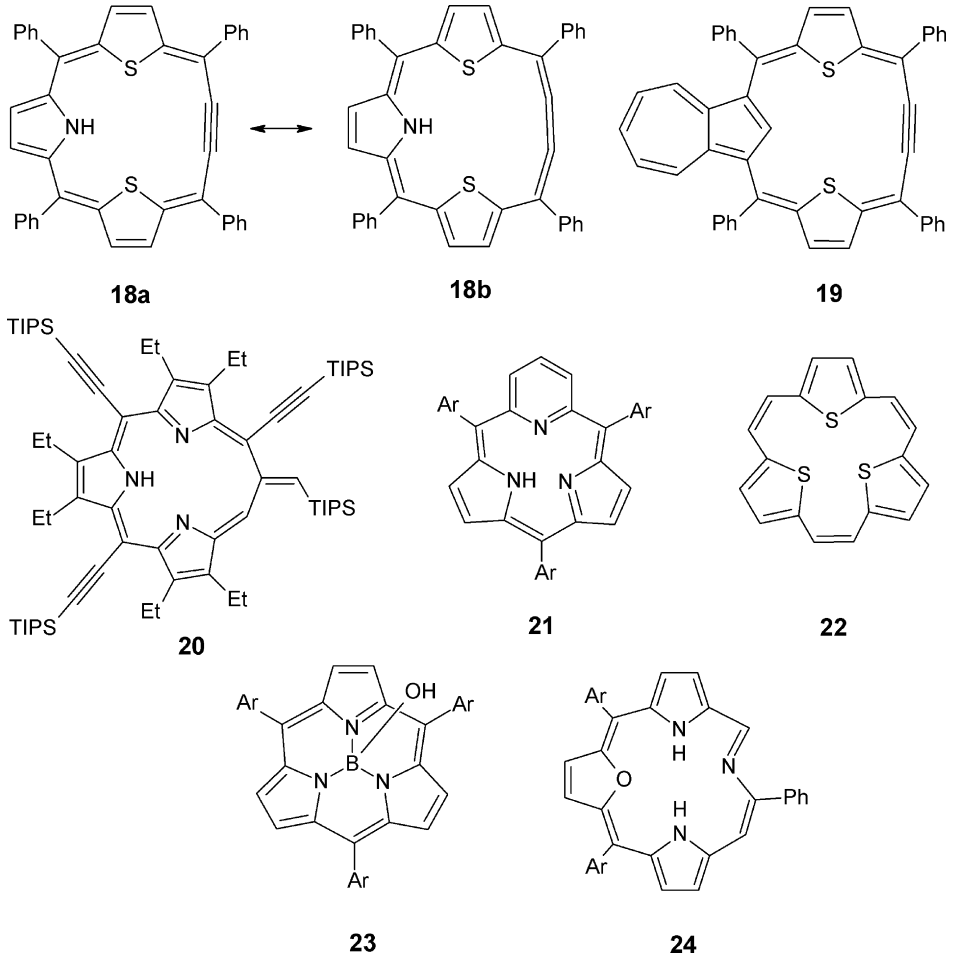

Pyrrole replaced by an acyclic moiety. An acetylenic carbon chain as a construction element of porphyrinoids has been employed to enlarge these macrocycles [50,51]. In triphyrin **18**, one pyrrole is replaced by the –C≡C– element which is given a chance to get close to a coordinated metal ion [42]. This atypical ligand, capable of binding a ruthenium ion, incorporates butyne moiety which reveals acetylene–cumulene character. In the ruthenium complex the acetylenic moiety is held close to the acetylenic fragment, but is not involved in coordination. Similar acetylenic macrocycle **19**, where a pyrrole is replaced by azulene, acts as a organometallic ligand with a contracted (as compared to a porphyrin) coordination core. This molecule, together with carbacorrole [52], N-confused corrole [53] and P-confused phosphacorrole [54] are the only contracted carbaporphyrins up to date.

2.6. E/Z isomerism in a porphyrinoid skeleton

In certain conditions an annulene-like conformational flexibility of vacataporphyrin is observed. It may be reduced to *E*/*Z* isomerism (*vide infra*) of the built-in butadiene moiety. The occurrence of *E*/*Z* isomerism, besides already mentioned large vinylogous porphyrins, has been noticed in the three-carbon *meso*-link of isoporphycene [porphyrin(3.0.1.0)] **25** [55,56]. An insertion of palladium(II) to isoporphycene results in the mixture of two stereoisomers, **25**(***Z***)-**Pd** and **25**(***E***)-**Pd**, which are mutually convertible due to exposure to light.

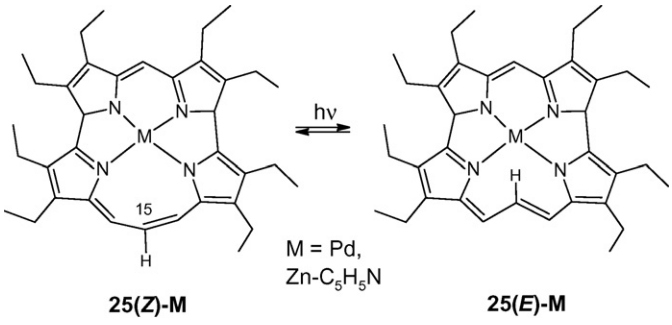

The composition of the mixture varies depending on the light conditions ((*Z*):(*E*) from 40:60 to 50:50). The isomerization is easy to track by ^{1}H NMR spectroscopy using the H15 resonance as a structural probe. Following the (*Z*) to (*E*) transformation the H15 proton relocates from the outside into the shielding zone and its signal moves from 9.42 to −3.26 ppm. The resemblance of these chemical shifts to that of an annulene: all *cis*-cyclononatetrenyl anion and its *cis*, *cis*, *cis*, *trans* isomer was noted.

The *Z*/*E* isomerism of this type is also characteristic for a stretched porphyrin of a deltoid shape, i.e. [22] porphyrin(3.1.1.3) **26** [22] with two adjacent bridging units longer than the other two. The macrocycle shows a very large diatropic ring current ($\Delta\delta \approx 23$ ppm). The geometries of the three-carbon bridges were established by ^{1}H NMR for the dication of **26**. Upon metallation with palladium(II) the macrocyclic framework was reorganized to accommodate the central ion and yielded **26**-**Pd**. Double *E*/*Z* isomerization of three-carbon units took place. The palladium(II) ion is held by three nitrogen atoms with chloride in the fourth coordination place, not in plane due to steric limitations.

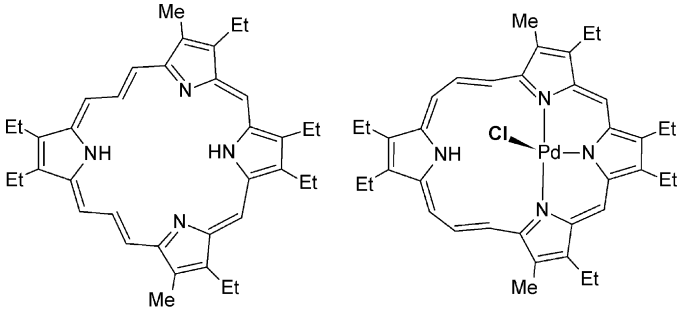

3. Vacataporphyrin

3.1. Synthesis

Formally vacataporphyrin [1] can be constructed from a porphyrin merely by extrusion of NH bridging group followed by addition of two hydrogen atoms. Actually 5,10,15,20-tetraaryl-21-telluraporphyrin [57] **27** was used as the precursor to form 5,10,15,20-tetraaryl-21-vacataporphyrin **1** in the reaction with concentrated hydrochloric acid (Scheme 1).

The replacement of HCl by DCl yields a deuterated derivative of **1** where deuterium atoms are bound to C1 and C4 (formerly α-tellurophene carbon atoms) and to some extent are located at β-pyrrolic positions. The partially deuterated derivatives of **1** were important in unambiguous assignments of analytically significant ^{1}H NMR resonances of metallovacataporphyrins.

3.2. Properties

Vacataporphyrin has been characterized by X-ray crystallography (Fig. 1). The macrocyclic ring is nearly planar resembling the parent telluraporphyrin **27**.

The planar and rigid structure of **1**, detected in solid, is preserved in the solution as determined by ^{1}H NMR. The resonances assigned to the butadiene moiety, located at the downfield and

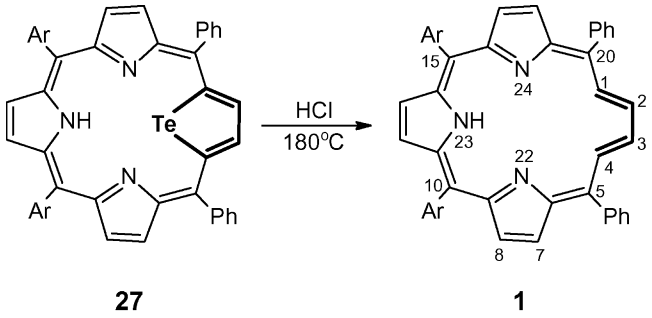

Scheme 1. Formation of vacataporphyrin.

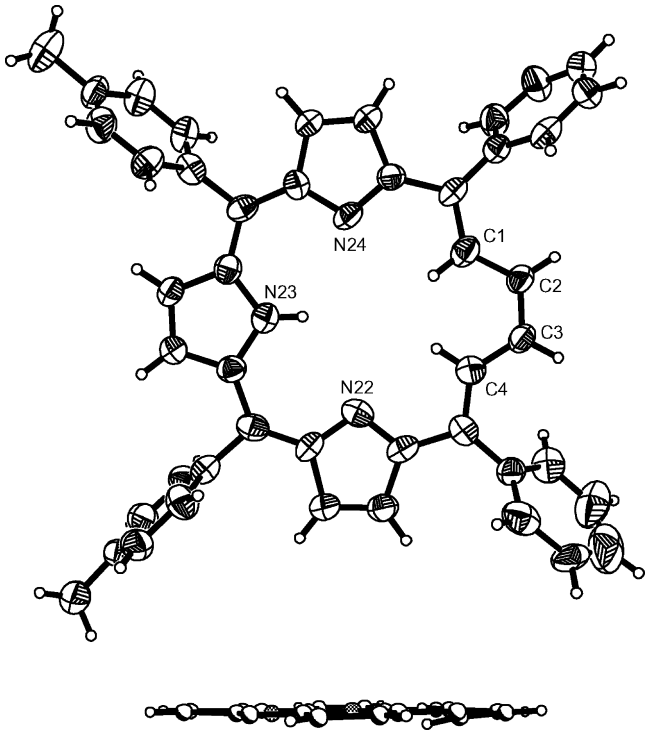

Fig. 1. The crystal structure of **1** (top: perspective view, vibrational ellipsoids represent 50% probability; bottom: side view, *meso*-aryls omitted for clarity). Copyright Wiley–VCH Verlag GmbH & Co. KGaA. Reproduced with permission from Ref. [1].

upfield regions of the spectrum ($\delta_{1,4} = -2.50$, $\delta_{2,3} = 9.65$) are consistent with the aromatic structure. Remarkably, these ^{1}H NMR parameters of **1** match those of [18]annulene [58,59]. On the other hand the ^{1}H NMR spectrum of the pyrrolic part of vacataporphyrin presents the δ and J values which are typical for 5,10,15,20-tetraaryl-21-heteroporphyrins [25].

3.3. Vacataporphyrin conformers; DFT calculations

Although a planar conformation of vacataporphyrin was observed, in light of flexibility of ditelluraporphyrin **16** and parabenziporphyrin **15**, several different geometries of **1** were analyzed [60]. The starting point of visualization of possible vacataporphyrin conformers is to consider separately two parts of the molecule (referring to its triphyrin(6.1.1) nature): the rather rigid tripyrrin "holder", although allowing some limited degree of flexibility, and the annulenic six-carbon bridge. For the latter, which is expected to be very flexible, several conformational and configurational possibilities are depicted in Scheme 2, described by (*Z*) or (*E*) configurations of each of five bonds although this geometry has to be adjusted to the tripyrrin spacing and *meso*-aryl steric hindrance.

The geometries resulting from amalgamation of tripyrrin and butadiene moieties were subject to DFT optimization at the B3LYP/6–31G** level of theory. The final B3LYP geometries, for which the genuine energy minimum was obtained, are shown in Fig. 2.

The calculated total energies (Table 1) demonstrate that the planar conformer is the most stable that accounts for the preference for $\mathbf{1_A}$ (*EEZEE*) structure in the solution and in the solid state. The relative energy of conformers increase in the series $\mathbf{1_A} < \mathbf{1_B} < \mathbf{1_C} \leq \mathbf{1_F} < \mathbf{1_E} < \mathbf{1_D}$. Five ($\mathbf{1_A}$, $\mathbf{1_B}$, $\mathbf{1_C}$, $\mathbf{1_D}$ and $\mathbf{1_E}$) out of six considered geometries of **1** were captured by metal ion coordination.

The vacataporphyrin as an 18-π-electron system is expected to be aromatic according to the Hückel's rule, unless a severe ruffling

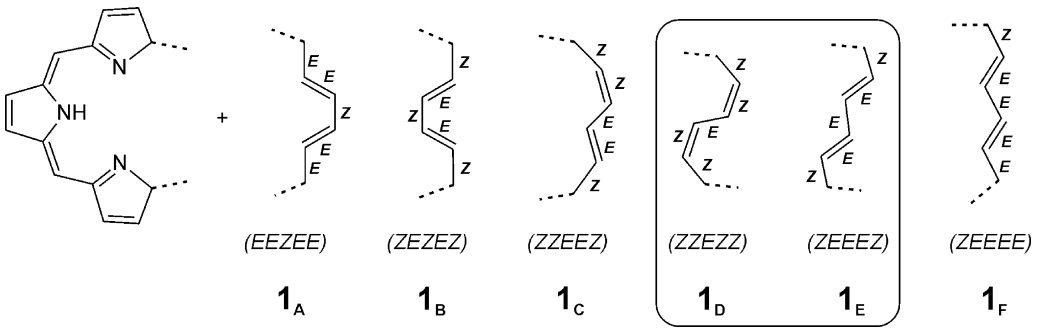

Scheme 2. Building blocks of vacataporphyrin (locations of linkage in dashed line): the tripyrrin and different isomers of the six-carbon bridge. Bridges forming the Möbius molecular band in frame. Adapted with permission from Ref. [60]. Copyright 2008 American Chemical Society.

of the macrocycle prohibits without a sufficient conjugation, forcing non-aromaticity. At the same time one needs to have in mind that the Hückel's rule is not valid for annulenes in twisted conformations, where the p orbitals lie on the surface of a Möbius strip. For such systems the [4*n*]annulenes would be aromatic and [4*n* + 2]annulenes–antiaromatic, as Heilbronner theoretically predicted in 1964 [61]. In fact Möbius annulenes emerged only recently as stable compounds, commencing from the spectacular work of Herges in 2003 [62,63], followed by discoveries in expanded porphyrinoid field by Latos-Grażyński's [60,64] and Osuka's groups [65,66].

In the "Möbius annulenes" a 180° twist of the ring, necessary to obtain a Möbius band π system, is achieved by combining normal and in-plane conjugations. Two cases of Möbius topology were recognized among the conformers of **1**, namely $\mathbf{1_D}$ and $\mathbf{1_E}$. The construction of vacataporphyrin isomers of this type is schematically outlined in Fig. 3, trace A, representing the example of isomer $\mathbf{1_D}$. The tripyrrin fragment mean plane (normal conjugation) forms a 90° angle with the butadiene moiety plane (in plane conjugation). The second Möbius form, $\mathbf{1_E}$ is constructed in the same manner, simply from a different isomer of the six-carbon bridge. One can readily notice that an alternative mode of tripyrrin and butadiene

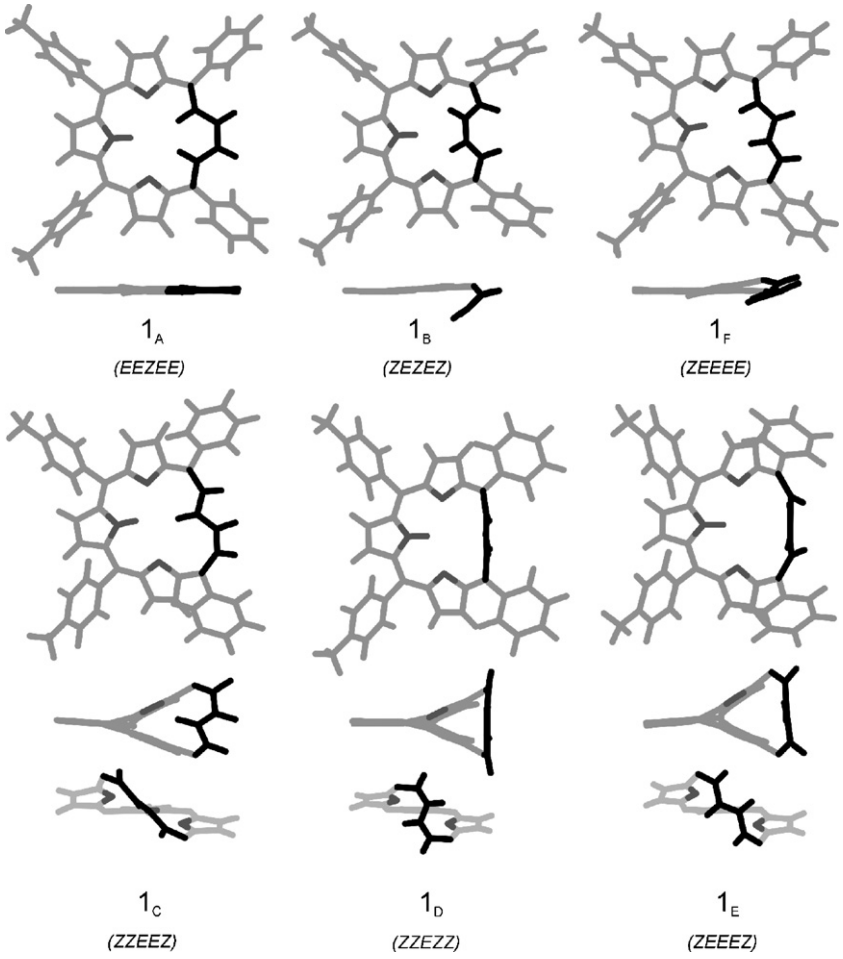

Fig. 2. Geometries of vacataporphyrin stereoisomers obtained in a DFT optimization for level B3LYP/6–31G**. Projections emphasize the conformations of macrocycle. Configurations of six-carbon bridge in parentheses. Adapted with permission from Ref. [60]. Copyright 2008 American Chemical Society.

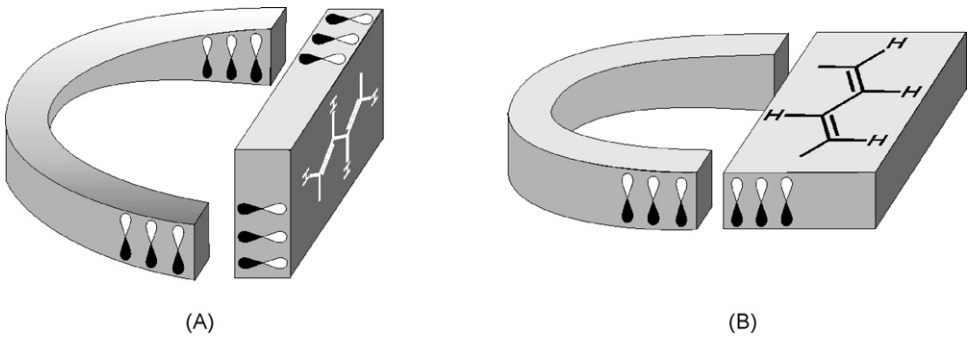

Fig. 3. Strategy to construct (A) Möbius and (B) Hückel conformers of vacataporphyrin. Reproduced with permission from Ref. [60]. Copyright 2008 American Chemical Society.

Table 1
Relative energies and nucleus-independent chemical shift (NICS) for vacataporphyrin and palladium(II) vacataporphyrin conformers [60]. Möbius isomers shadowed.

Vacataporphyrin conformation	$\mathbf{1_A}$	$\mathbf{1_B}$	$\mathbf{1_C}$	$\mathbf{1_D}$	$\mathbf{1_E}$	$\mathbf{1_F}$
E[a] of $\mathbf{1_X}$	**0**	7.02	8.05	19.68	14.05	8.18
NICS[b]	−13.6	−7.5	−7.7	+6.0	+4.0	−11.7
E[c] of $\mathbf{1_X}$**-Pd**	15.12	5.96	-	**0**	6.21	-

[a]Energy relative to $\mathbf{1_A}$, kcal/mol, calculated using the B3LYP/6–31G**// B3LYP/6–31G** approach.
[b]NICS in ppm, calculated by GIAO-B3LYP method for B3LYP/6–31G** geometries.
[c]Energy relative to $\mathbf{1_D}$**-Pd**, kcal/mol, calculated using the B3LYP/LANL2DZ// B3LYP/LANL2DZ approach.

connections (both fragments are located in approximately parallel planes) creates a molecule acquiring the Hückel topology (Fig. 3, trace B), as in $\mathbf{1_A}$, $\mathbf{1_B}$, $\mathbf{1_C}$ and $\mathbf{1_F}$.

The analysis of the topology of the above vacataporphyrin structures is based on the number of half-twists in the ring. Alternatively the topology can be determined by counting the number of trans (*E*) bonds along the conjugation pathway. The odd number indicates Möbius systems, even—Hückel-rule annulenes (Scheme 2, Fig. 2).

The 18-π electron vacataporphyrin isomers of Möbius topology, may be antiaromatic, if the orbital overlapping in the ring is sufficient for effective π-conjugation (a limit of 50° is put on the torsion angles). Calculations of the nucleus-independent chemical shifts (NICS), computational measure of aromaticity related to experimental magnetic criteria, have been performed for 17-membered central rings of all vacataporphyrin conformers (Table 1). The positive NICS values, +6 and +4 for $\mathbf{1_D}$ and $\mathbf{1_E}$ respectively, are in accord with the expected antiaromatic character. Actually the experimental observation of those Möbius topologies was possible for palladium(II) complexes [60].

4. Vacataporphyrin complexes

Vacataporphyrin, with its 17-atom coordination core, slightly larger than in N_4 porphyrins(1.1.1.1) binds efficiently metal ions. A central metal ion is bound in the macrocyclic cavity by three pyrrolic nitrogen atoms. Such coordination imposes steric constraints on the ligand geometry and leads to stereoisomers with the annulene part adopting several configurations. Consequently the annulene part is exposed to coordination or interaction with metal ions.

4.1. Planar isomer

Vacataporphyrin reacts with cadmium(II), zinc(II), nickel(II) and palladium(II) affording tetracoordinate complexes **1-M** [60,67]. If the reaction is carried in the dark, the basic form of the complex i.e., resembling in shape the free ligand $\mathbf{1_A}$, prevails (Scheme 3). The isomer $\mathbf{1_A}$**-M** is exclusively obtained solely for palladium(II). In this form the macrocycle acts as a monoanionic ligand coordinating through the three nitrogen donors. To complete the coordination sphere of metal dication one additional chloride ligand is required. For the palladium complex, the X-ray structure was obtained (Fig. 4).

The geometry of the complex reflects the balance among constraints of the macrocycle ligand, the size of the palladium ion, and the predisposition of the palladium for square planar geometry. The distinct features of the structure are the very pronounced bending of the chloride ligand toward the annulenic unit and the planar (approximately) butadiene moiety displaced below the C_{meso} plane (C5–C10–C15–C20) as a consequence of strain induced by incorporation of a metal-chloride bond into a macrocycle with a limited core. A similar coordination geometry is observed for the deltoid shape porphyrin vinylog palladium complex [22]. The bond distances within the tripyrrolic and annulenic framework of $\mathbf{1_A}$**-Pd** indicate that the macrocycle is highly conjugated following the free base pattern. The evidence of the $\mathbf{1_A}$**-M** aromaticity comes from ^{1}H NMR studies of palladium(II), zinc(II) and cadmium(II) complexes. Their spectral patterns are similar to that of a free base suggesting that the basic structural features of $\mathbf{1_A}$ are preserved after metal ion insertion. The ^{1}H NMR signals of H1–H4 protons can be treated as fingerprints of the annulene moiety, tracing its conformation reflected in coupling constants values, and at the same time being a base of an aromaticity probe ($\Delta\delta$). The resonance of external H2, H3 is located in downfield, and internal H1, H4—in upfield regions of the spectrum. The $\Delta\delta = \delta_{H2} - \delta_{H1}$ values vary from 12.15 ppm for $\mathbf{1_A}$, 10.77 for $\mathbf{1_A}$**-Cd**, 9.28 for $\mathbf{1_A}$**-Zn** and finally 8.01 for $\mathbf{1_A}$**-Pd**. (Fig. 5). The weakened aromatic current of $\mathbf{1_A}$**-M** suggests some nonplanarity imposed by coordination.

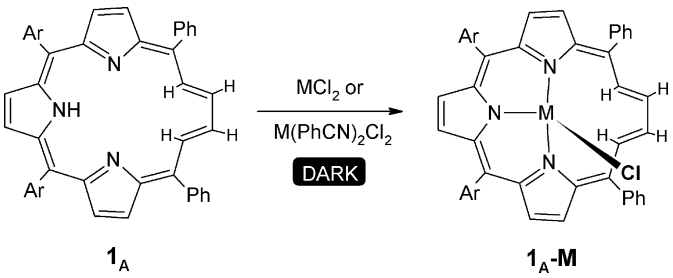

Scheme 3. Metallation of a vacataporphyrin.

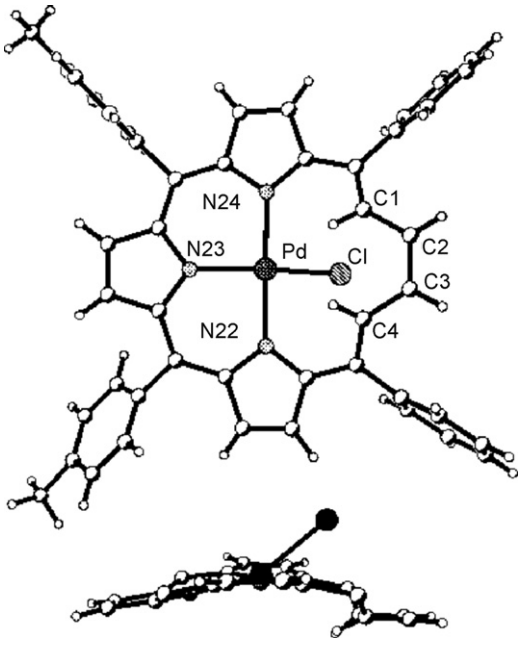

Fig. 4. The crystal structure of $\mathbf{1_A}$-**Pd** (top: perspective view, bottom: side view; phenyl groups omitted for clarity). The thermal ellipsoids represent 50% probability. Reproduced with permission from Ref. [60]. Copyright 2008 American Chemical Society.

Specifically for cadmium(II) vacataporphyrin an additional ^{1}H NMR probe is available. Namely scalar couplings of protons with the $^{111/113}$Cd spin-active nuclei have been used to detect a unique cadmium-butadiene interaction. Significantly the "through space" couplings between $^{111/113}$Cd and H1, H4 prove their spatial proximity.

4.2. Photochemical isomerization, bent isomer

In solution cadmium(II) and zinc(II) vacataporphyrins exist as inseparable mixtures of two stereoisomers. In addition to the already described $\mathbf{1_A}$-**M** a new isomer $\mathbf{1_B}$-**M**, containing the bent butadiene moiety as considered for $\mathbf{1_B}$, has been identified. The $\mathbf{1_A}$-**M** → $\mathbf{1_B}$-**M** transformation is induced by light and involves a flip of annulene bridge that transfers the C2–C3 unit from the periphery towards the macrocyclic center (Scheme 4). This profound structural transformation was observed only for a coordinated vacataporphyrin and exemplifies its unusual structural flexibility triggered by coordination.

The relative abundance of $\mathbf{1_A}$-**M** and $\mathbf{1_B}$-**M** depends on the exposure to light. The isomerization is reversible and proceeds slowly. The molecular ratio [$\mathbf{1_A}$-**Cd**]:[$\mathbf{1_B}$-**Cd**] as monitored by ^{1}H NMR changed in a chloroform solution (RT) between the values of 5:2,

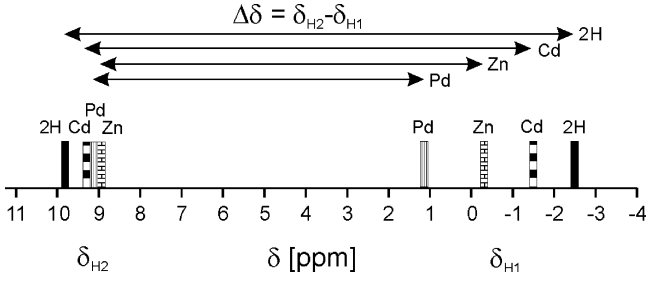

Fig. 5. Schematic representation of the diagnostic, inner (H1) and outer (H2) annulene hydrogens chemical shifts and Δδ of different $\mathbf{1_A}$-**M** vacataporphyrin complexes.

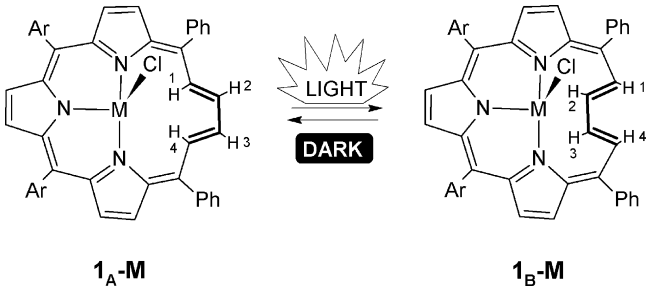

Scheme 4. Photochemical isomerization of vacataporphyrin complexes. M = Cd(II), Zn(II).

when stored in the dark and 1:6 after the exposition to daylight. The comparable concentrations of both isomers raised the question of their relative thermodynamic stability. Both isomers $\mathbf{1_A}$-**Cd** and $\mathbf{1_B}$-**Cd** were subject to geometry optimization and relative energy calculations using the density-functional theory (DFT) methods (B3LYP/LANL2DZ). The small energy difference between $\mathbf{1_A}$-**Cd** and $\mathbf{1_B}$-**Cd** (2.3 kcal/mol) accounts for their simultaneous presence.

For $\mathbf{1_B}$-**Cd** the $^{111/113}$Cd satellites were detected for all the H1, H2, H3 and H4 hydrogens, attributed to $^{111/113}$Cd···(C–H) "through space" interaction, proving the spatial adjacency of the cadmium(II) ion and the butadiene fragment. The side-on location of cadmium(II) with respect to the butadiene fragment in the folded structure of $\mathbf{1_B}$-**Cd** affords the simultaneous contacts with all C–H and C–C units of butadiene. The DFT-calculated cadmium–proton distances are equal 4.14 and 3.19 Å for H1 and H2 respectively.

The ^{1}H NMR spectra of $\mathbf{1_B}$-**M** differ markedly from those collected for their $\mathbf{1_A}$-**M** counterparts. In particular they reveal diametrical relocations of the crucial H1, H2, H3 and H4 resonances as compared to $\mathbf{1_A}$-**M**. The H2, H3 hydrogens of $\mathbf{1_B}$-**M** are located in the shielding zone, H1, H4—in the deshielding zone of the diatropic ring current. Actually the small shift differences in the butadiene fragment ($\Delta\delta$ = 2.69 ppm for $\mathbf{1_B}$-**Cd** and $\Delta\delta$ = 1.16 ppm for $\mathbf{1_B}$-**Zn**) reflect the weak aromatic current and correspond with marked nonplanarity of this macrocycle. Thus $\mathbf{1_B}$-**M** complexes exemplify the borderline cases of porphyrinoid aromaticity.

The highly nonplanar structure of $\mathbf{1_B}$-**M** with an inverted conformation of the annulene fragment has precedence in 21,23-ditelluraporphyrin **16** [38]. The relevant structural motive can be also seen in an appropriate reference model i.e. in the structure of cadmium(II) *p*-benziporphyrin **15**-**M** (Scheme 5). For instance a dihedral angle between butadiene moiety and the N_3-plane (45.2°) in $\mathbf{1_B}$-**Cd** (DFT) is similar to the analogous dihedral phenylene/N_3-plane angle (45°) determined for cadmium(II) *p*-benziporphyrin (X-ray), **15**-**Cd** [36].

4.3. Paramagnetic nickel(II) complexes

Owing to the nonplanar coordination geometry of the metal ion, the nickel(II) complex of vacataporphyrin **1**-**Ni** is paramagnetic (S = 1) and its ^{1}H NMR characteristics is quite typical for high-spin nickel(II) complexes of porphyrin analogues [25]. Similarly as described for diamagnetic cadmium(II) and zinc(II) complexes, **1**-**Ni** is a mixture of two conformers: $\mathbf{1_A}$-**Ni** and $\mathbf{1_B}$-**Ni**. The $\mathbf{1_A}$-**Ni** → $\mathbf{1_B}$-**Ni** transformation is induced by light but in contrast to cadmium(II) and zinc(II) vacataporphyrins the photochemical isomerization could not be reversed.

4.3.1. Conformational flexibility of the planar isomer

The two stereoisomers $\mathbf{1_A}$-**Ni** and $\mathbf{1_B}$-**Ni** coexisting in solution reveal a different conformational flexibility. The variable temperature ^{1}H NMR studies of $\mathbf{1_A}$-**Ni** and $\mathbf{1_B}$-**Ni** demonstrated the unusual temperature dependence of the line widths of $\mathbf{1_A}$-**Ni** allowing to

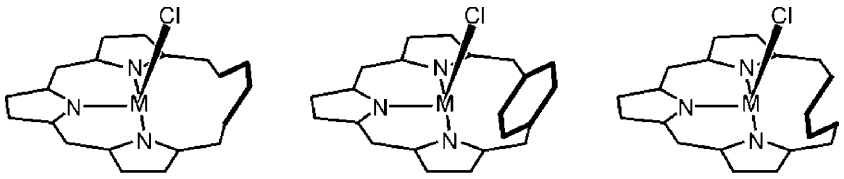

Scheme 5. Two stereoisomers of **1**-**M** compared with *p*-benziporphyrin complex **15**-**M**. Adapted with permission from Ref. [67]. Copyright 2005 American Chemical Society.

conclude that **1$_A$**-**Ni** is involved in an intramolecular dynamic process. By contrast in identical conditions **1$_B$**-**Ni** is not involved in any chemical exchange. The observed behaviour was interpreted in terms of an equilibrium in which one of the forms, **1$_{AA}$**-**Ni**, is present at a very small concentration and cannot be observed directly (Scheme 6).

4.3.2. Five-coordinate complexes

The marked differences in ^{1}H NMR spectra of **1**-**Ni** in methanol-d_4 or acetonitrile-d_3 as compared to chlorinated solvents are attributed to an axial coordination of two solvent molecules with formation of single forms of **1**-**Ni**$(CD_3OD)_2^+$ or **1**-**Ni**$(CD_3CN)_2^+$ respectively. Actually the **1$_A$**-**Ni** and **1$_B$**-**Ni** stereoisomers have different affinity for the second axial ligand as revealed during the titration with [$BzPh_3P$]Cl (benzyltriphenylphosphonium chloride). In **1$_B$**-**Ni** the bent butadiene fragment adjacent to the nickel(II) ion blocks sterically one side of the porphyrin and binding of the second chloride is slower than for **1$_A$**-**Ni**. Besides a unique spectroscopic pattern of these bis-axial complexes, an additional proof was obtained in the case of imidazole coordination, where the axial ligands were directly identified and showed paramagnetically shifted signals (Fig. 6). The number and relative intensities of the imidazole resonances indicate that two axial ligands are bound and both sides of vacataporphyrin are equivalent. Therefore the only possible macrocyclic conformation in bis-axial complexes is the planar one.

4.4. Palladium(II) complexes

Coordination of palladium(II) to three pyrrolic nitrogens of vacataporphyrin triggers a unprecedented sequence of conformational changes, which have been readily visualized by ^{1}H NMR spectroscopy as the respective spectra reflect distinct diatropic or moderate paratropic effects. The control over the isomerization processes has been achieved by manipulating with the light presence, an acid concentration and axial ligand strength.

4.4.1. Complex with metal–carbon bond

1$_A$-**Pd** complex exposed to light did not yield an **1$_B$**-**Pd** isomer, expected by analogy to the cadmium(II) chemistry, but a new aromatic species **1$_C$**-**Pd** was solely produced. This is the first complex where vacataporphyrin acts as a dianionic organometallic ligand, with unprotonated trigonally hybridized C2 carbon (Scheme 7). The

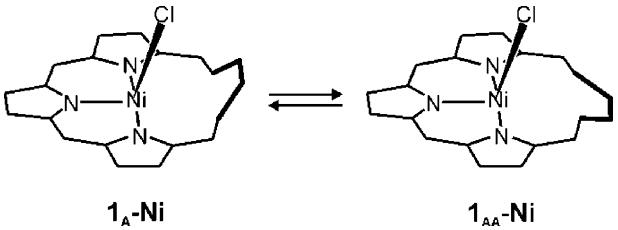

Scheme 6. Conformational equilibrium involving the **1**-**Ni** extended isomers. Adapted with permission from Ref. [67]. Copyright 2005 American Chemical Society.

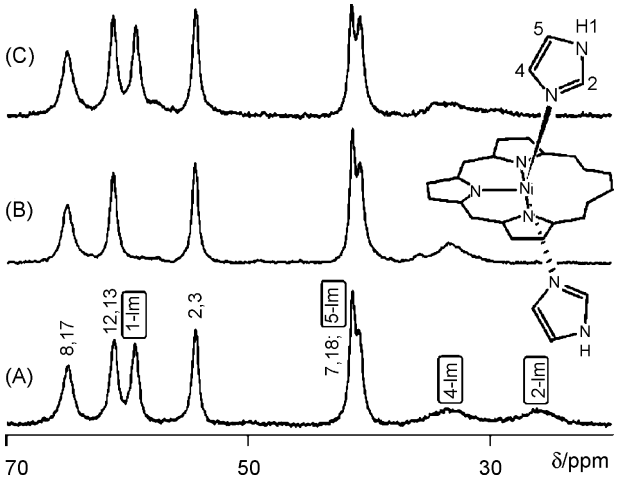

Fig. 6. ^{1}H NMR ($CDCl_3$, 298 K) spectra of **1**-**Ni** solution in the presence of (A) imidazole, (B) imidazole-1,2-d_2, and (C) imidazole-2,4,5-d_3. The molar ratio **1**-**Ni:** imidazole 1:2.5. Reproduced with permission from Ref. [67]. Copyright 2005 American Chemical Society.

palladium(II) ion is located in the plane of the butadiene fragment and does not require an axial chloride. The complex contains the dianionic macrocyclic ligand directly derived from **1$_C$** by dissociation of H2 and H23 protons

The **1$_A$**-**Pd** → **1$_C$**-**Pd** reaction route does not include the transient **1$_B$**-**Pd** species as it proceeds with well-defined isosbestic points recorded in the UV–vis electronic spectroscopy. ^{1}H NMR spectrum of **1$_C$**-**Pd** is in accord with its aromatic nature and lack of any symmetry element. Analysis of coupling constants and chemical shifts established that the configuration of the annulene fragment of **1$_C$**-**Pd** matches the hypothetical conformation of **1$_C$**.

4.4.2. Isomers of Möbius band topology

The most exciting result in the vacataporphyrin complexes investigation is the discovery of some forms of a rare Möbius strip topology that have a $(4n+2)$ π-electron conjugated system and reveal a measurable paratropicity. Of particular importance is the

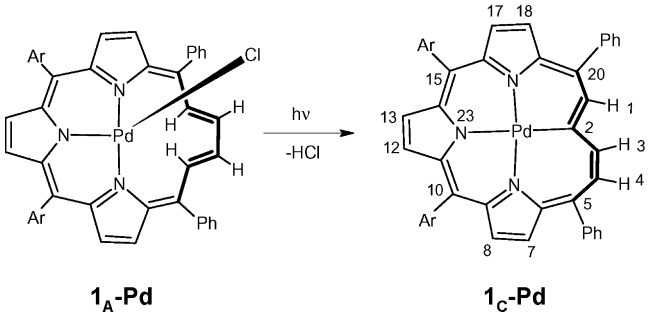

Scheme 7. Formation of vacataporphyrin complex with a carbon–palladium(II) bond.

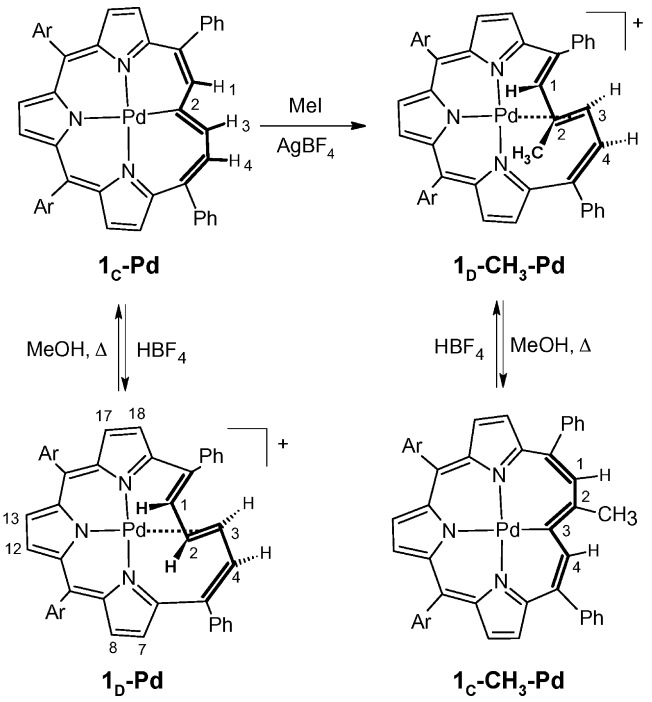

Scheme 8. Alkylation and protonation of **1_C-Pd**. Adapted with permission from Ref. [60]. Copyright 2008 American Chemical Society.

observation that **1_C-Pd** is susceptible to methylation or protonation at the C2 atom. Thus **1_C-Pd** rapidly reacts with MeI/$AgBF_4$ to yield a unique organopalladium(II) complex **1_D-CH_3-Pd** (Scheme 8). Analogous non-methylated **1_D-Pd** has been generated by regioselective protonation of **1_C-Pd** carried out by addition of strong acids (HBr/CH_3COOH or HBF_4/Et_2O in anhydrous conditions). Thus the hypothetical conformer **1_D** of vacataporphyrin has been successfully trapped by palladium(II) coordination.

The structure of **1_D-Pd** is strongly folded and contains an S-like C20–C1–C2–C3–C4–C5 structural motif. The C2–C3 bond is oriented perpendicularly to the N_3 plane (90° angle was obtained from the DFT model) and acquires a typical orientation of the η^2-alkene coordinated to palladium(II) in square planar complexes with a –C=C– moiety. Such a conformation of **1_D-Pd** allows the palladium(II) η^2 interaction with C2–C3, which affords observed ^{13}C NMR coordination shifts of C2 and C3 carbons (38 ppm, referred to **1_A-Pd**). The definitive proofs of the molecule shape come from ^1H NMR spectroscopy. Thus NOE effects connect spatially the methyl group of **1_D-CH_3-Pd** with protons on the opposite side of the molecule. The J_{H-H} coupling constants in the butadiene moiety are consistent with its (*ZZEZZ*) configuration. The essential spectroscopic feature is the paratropic ring current effect detected in this system. This observation together with the π-electron count of 18 is accord with the Möbius topology of the conjugation pathway. **1_D-Pd** complex gives ^1H NMR spectrum (Fig. 7) with β-H signals shifted upfield relative to non-aromatic fully conjugated pyrrolic systems. The reversed order (relative to aromatic systems) of *meso*-phenyl resonances has been observed (*para*-H > *meta*-H > *ortho*-H). The peculiar position of the methine H2, H3 resonance at 8.98 pm has also been noted. For the methylated derivative, **1_D-CH_3-Pd** the paratropic effect is present although evidently smaller and the number of resonances is doubled due to the lower symmetry.

The protonation of **1_D-Pd** is reversible. Thus heating the solution of **1_D-Pd** with addition of methanol recovers **1_C-Pd** (Scheme 8). An analogous deprotonation of **1_D-CH_3-Pd** follows a similar path producing the appropriate C-methylated aromatic derivative **1_C-CH_3-Pd**. The presented reactions create a chain of transformations: **1_A-Pd** → **1_C-Pd** → **1_D-Pd** (Schemes 7 and 8) which require a series of profound structural rearrangements. The changes involve primarily the six-carbon annulene fragment.

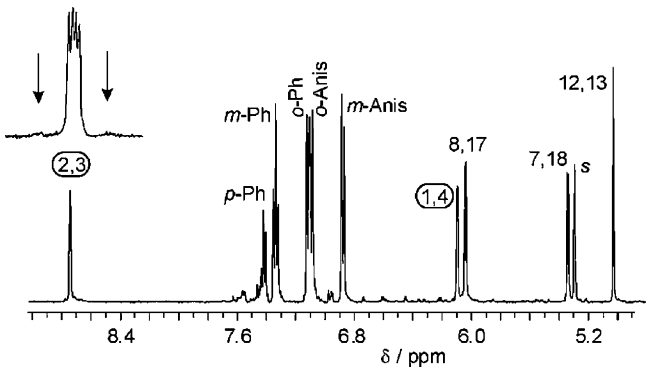

Fig. 7. ^1H NMR spectrum (CD_2Cl_2, 298 K, Ar = Anis) of **1_D-Pd**. Resonance assignments follow the numbering given in Scheme 8. Inset presents the details of the H2,3 multiplet. Adapted with permission from Ref. [60]. Copyright 2008 American Chemical Society.

*Alternative route to **1_D-Pd**.* Axial chloride of the maternal **1_A-Pd** may be subtracted by means of $AgBF_4$ addition, carried out in the dark, in $CDCl_3$ solution. Subsequently water, present in the medium in trace amounts, occupies the created vacancy and a labile water-coordinated **1_A-Pd**$(H_2O)^+$ complex is formed, which transforms in ca. 3 min (293 K) to another intermediate, **1_E-Pd**, which finally, after about 4 h, decays irreversibly to **1_D-Pd**. Apparently the fourth coordination position of **1_A-Pd**$(H_2O)^+$ becomes available to be occupied by C2–C3 moiety after facile dissociation of the bound water molecule (Scheme 9). The time of decay of **1_E-Pd** can be hastened to few minutes by presence of light.

As a final point it has been demonstrated that the second conformer of Möbius topology **1_E** has been trapped as the palladium(II) complex **1_E-Pd**. In this case the zigzag shape of C20–C1–C2–C3–C4–C5 orients the central C2–C3 fragment coplanarly with the PdN_3 plane filling the fourth corner of the square-planar structure. **1_E-Pd** reveals a weak η^2-Pd–(C2–C3) interaction. The ^1H NMR spectrum of **1_E-Pd** resembles the basic features of **1_D-Pd** (Figs. 7 and 8) consistent with Möbius antiaromaticity albeit the effect is markedly less pronounced (for **1_E-Pd** $\delta_{H2}-\delta_{H1}$ = 1.63 ppm, **1_E-Pd**: 2.67 ppm). Again the observed chain of transformations **1_A-Pd** → **1_E-Pd** → **1_D-Pd** leads from the maternal **1_A** to Möbius **1_D** structure. That raised a question of relative stabilities of the described palladium(II) vacataporphyrins.

4.4.3. DFT studies of palladium vacataporphyrin complexes

Density-functional theory studies were performed for palladium(II) vacataporphyrin complexes. The structures without axial ligand (i.e. cations, except neutral **1_C-Pd**) were subjected to a DFT optimization (B3LYP/LANL2DZ) and final geometries

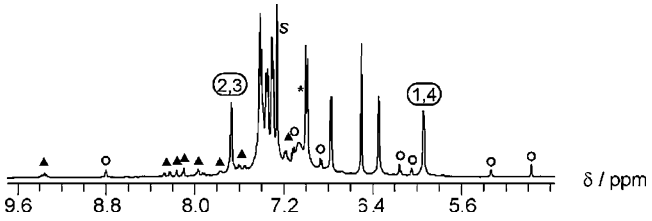

Fig. 8. ^1H NMR spectrum of **1_E-Pd** with traces of preceding and succeeding forms: **1_A-Pd** (triangle) and **1_D-Pd** (circle) (250 K, $CDCl_3$, Ar = Anis). Adapted with permission from Ref. [60]. Copyright 2008 American Chemical Society.

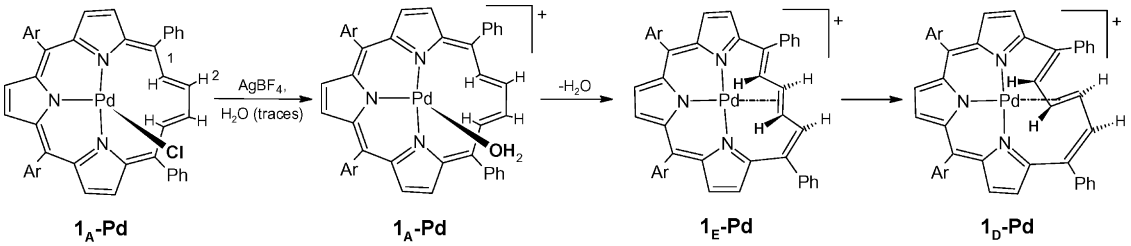

Scheme 9. Alternative route of $\mathbf{1_A}$-**Pd** into $\mathbf{1_E}$-**Pd** conversion. Adapted with permission from Ref. [60]. Copyright 2008 American Chemical Society.

corresponding to the detected $\mathbf{1_A}$-**Pd**, $\mathbf{1_C}$-**Pd**, $\mathbf{1_D}$-**Pd** and $\mathbf{1_E}$-**Pd** stereoisomers, together with hypothetical $\mathbf{1_B}$-**Pd** are shown in Fig. 9.

The energy ordering of **1-Pd** stereoisomers is: $\mathbf{1_D}$-**Pd** (0) < $\mathbf{1_B}$-**Pd** (5.96) ≤ $\mathbf{1_E}$-**Pd** (6.21) < $\mathbf{1_A}$-**Pd** (15.12 kcal/mol). Unexpectedly, the strongly folded Möbius strip structure of vacataporphyrin provides energetically the most favorable condition for palladium(II) coordination. Significantly the stability order is reversed in comparison to the free base vacataporphyrin (Table 1). In contrast to vacataporphyrin conformers the twisted structure $\mathbf{1_D}$-**Pd** can be considered as a fundamental state for the whole series. Thus the coordination of palladium(II) imposes additional structural constrains on vacataporphyrin and affords the remarkable stabilization of Möbius band geometries.

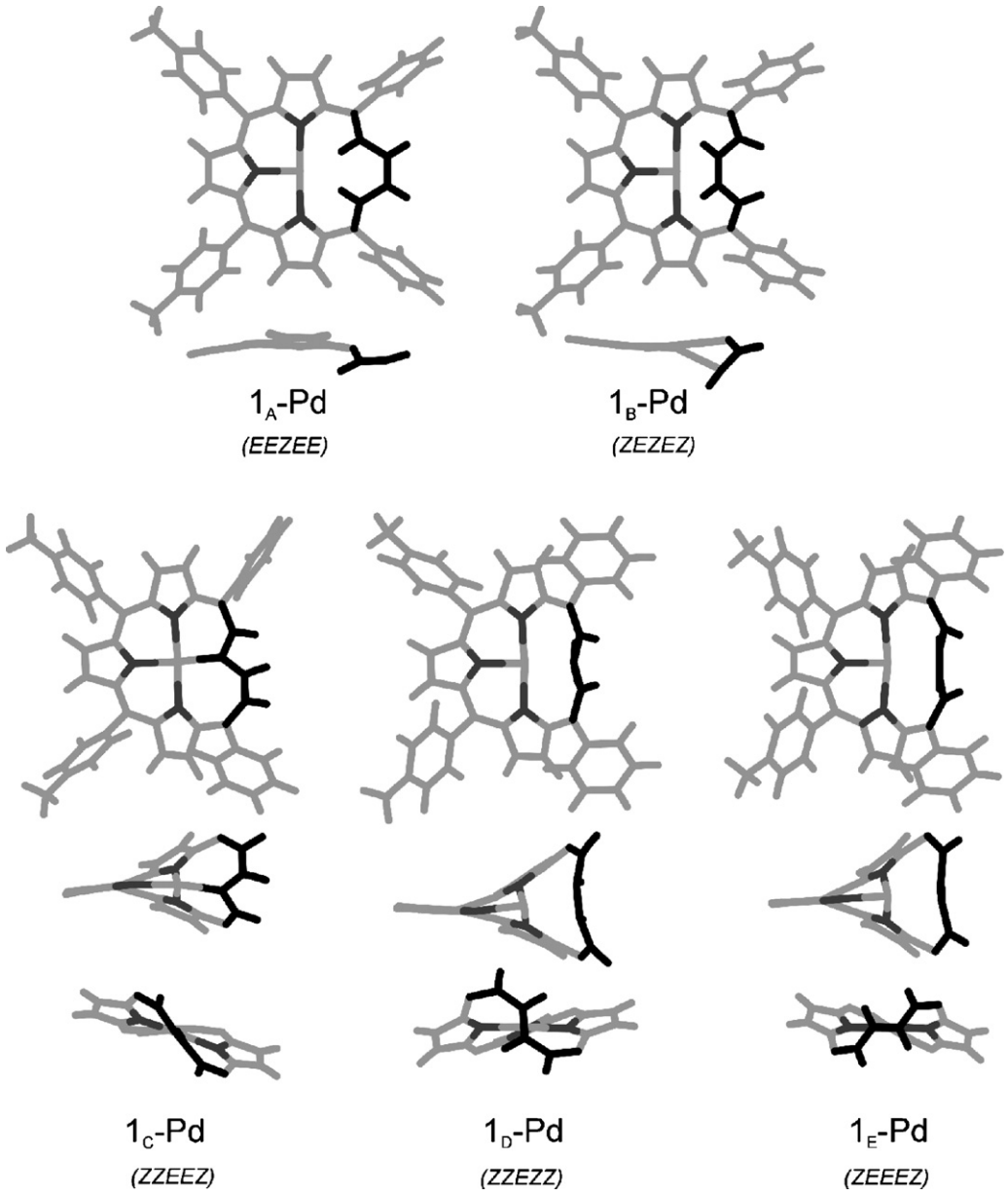

Fig. 9. Geometries of palladium vacataporphyrin complexes obtained in a DFT optimization (B3LYP/LANL2DZ). Projections emphasize the folding of the macrocycle. In parenthesis the configuration of C20–C1–C2–C3–C4–C5 fragment. Adapted with permission from Ref. [60]. Copyright 2008 American Chemical Society.

5. Conclusions

In summary, in this microreview we have shown that vacataporphyrin can be treated as an annulene–porphyrin hybrid. The macrocycle contains the relatively rigid tripyrrin moiety which affords the limited flexibility resembling regular porphyrins. In contrast the butadiene fragment can readily adopt several configurations consistent with the annulene-like nature of vacataporphyrin. Thus the combination of both structural components allows a unique flexibility of the whole conjugated macrocycle albeit constrained by tripyrrin fragment and eventually by coordination. Vacataporphyrin, applied as a ligand toward palladium(II), zinc(II), cadmium(II) and nickel(II) reveals the peculiar plasticity of its molecular and electronic structure. This important feature has enabled us to investigate and eventually to control the subtle interplay between their structural flexibility and aromaticity confining the butadiene moiety in a macrocyclic harness. In particular the coordinated vacataporphyrin may acquire the relatively planar Hückel or extremely rare twisted Möbius topologies which are reflected by aromatic or antiaromatic properties of 18-electron π-system respectively. Actually the very first example of Möbius antiaromaticity has been experimentally identified. Thus vacataporphyrin provides a stimulating environment to investigate coordination chemistry of the Möbius-type macrocyclic ligand. We are of opinion that this molecule provides a promising platform to explore a unique organometallic chemistry enforced by the proximity of the metal ion and the annulene fragment.

In the broader sense vacataporphyrin is the representative member of the larger class of molecules which are located on the cross-road of annulene–porphyrin chemistry. Here we have briefly mentioned the selected examples (norporphines, vinylogously enlarged porphyrins, tetraepoxy [32]annulenes(6.2.6.2), selected triphyrins, isoporphycene, a deltoid shape [22]porphyrin-(3.1.1.3)) of molecules which in our opinion share the aza-deficient porphyrin features. Consequently the studies on coordination chemistry of vacataporphyrin set the stage for the further exploration of the fascinating subject, i.e. on coordination chemistry of the annulene–porphyrin hybrids.

Acknowledgements

Financial support from the Ministry of Science and Higher Education (Grant PBZ-KBN-118/T09/2004) is kindly acknowledged.

References

[1] E. Pacholska, L. Latos-Grażyński, Z. Ciunik, Chem. Eur. J. 8 (2002) 5403.
[2] J.L. Sessler, T. Murai, V. Lynch, M. Cyr, J. Am. Chem. Soc. 110 (1988) 5586.
[3] C.-H. Lee, J.-W. Ka, D.-H. Won, Tetrahedron Lett. 40 (1999) 6799.
[4] J.L. Sessler, D. Seidel, Angew. Chem. Int. Ed. 42 (2003) 5134.
[5] J.L. Sessler, E. Tomat, Acc. Chem. Res. 40 (2007) 371.
[6] P.R. Ortiz de Montellano, J.P. Evans, N. Serradell, J. Bolos, E. Rosa, Drugs Future 32 (2007) 601.
[7] J.L. Sessler, R.A. Miller, Biochem. Pharmacol. 59 (2000) 733.
[8] E. Vogel, J. Heterocycl. Chem. 33 (1996) 1461.
[9] E. Vogel, Pure Appl. Chem. 65 (1993) 143.
[10] J. Waluk, J. Michl, J. Org. Chem. 56 (1991) 2729.
[11] J.-H. Fuhrhop, Angew. Chem., Int. Ed. Engl. 13 (1974) 321.
[12] M. Bohusch, W. Flitsch, H.-G. Kneip, Liebigs Ann. Chem. (1991) 67.
[13] W. Flitsch, Pure Appl. Chem. 58 (1986) 153.
[14] C.K. Chang, W. Wu, S.-S. Chern, S.-M. Peng, Angew. Chem., Int. Ed. Engl. 31 (1992) 70.
[15] K.R. Adams, R. Bonnett, P.J. Burke, A. Salgado, M.A. Vallés, J. Chem. Soc., Chem. Commun. (1993) 1860.
[16] C. Brückner, S.J. Rettig, D. Dolphin, J. Org. Chem. 63 (1998) 2094.
[17] C. Eickmeier, B. Franck, Angew. Chem., Int. Ed. Engl. 36 (1997) 2213.
[18] B. Franck, A. Nonn, Angew. Chem., Int. Ed. Engl. 34 (1995) 1795.
[19] M. Gosmann, B. Franck, Angew. Chem., Int. Ed. Engl. 25 (1986) 1100.
[20] E. LeGoff, O.G. Weaver, J. Org. Chem. 52 (1978) 710.
[21] E. Vogel, N. Jux, E. Rodriguez-Val, J. Lex, H. Schmickler, Angew. Chem., Int. Ed. Engl. 29 (1990) 1387.
[22] L. Xu, G.M. Ferrence, T.D. Lash, Org. Lett. 8 (2006) 5113.
[23] R. Paolesse, R. Khoury, F. Sala, C. Natale, F. Sagone, K.M. Smith, Angew. Chem. Int. Ed. 38 (1999) 2577.
[24] G. Märkl, R. Ehrl, H. Sauer, P. Kreitmeier, T. Burgemeister, Helv. Chim. Acta 82 (1999) 59.
[25] L. Latos-Grażyński, in: K.M. Kadish, K.M. Smith, R. Guilard (Eds.), The Porphyrin Handbook, vol. 2, Academic Press, New York, 2000, p. 361.
[26] P.J. Chmielewski, L. Latos-Grażyński, Coord. Chem. Rev. 249 (2005) 2510.
[27] I. Gupta, M. Ravikanth, Coord. Chem. Rev. 250 (2006) 468.
[28] Y. Matano, T. Nakabuchi, T. Miyajima, H. Imahori, H. Nakano, Org. Lett. 8 (2006) 5713.
[29] J.D. Harvey, C.J. Ziegler, Coord. Chem. Rev. 247 (2003) 1.
[30] M. Stępień, L. Latos-Grażyński, Acc. Chem. Res. 8 (2005) 88.
[31] M. Pawlicki, L. Latos-Grażyński, Chem. Rec. 6 (2006) 64.
[32] H. Maeda, H. Furuta, Pure Appl. Chem. 78 (2006) 29.
[33] T.D. Lash, Eur. J. Org. Chem. (2007) 5461.
[34] M. Stępień, L. Latos-Grażyński, L. Szterenberg, J. Panek, Z. Latajka, J. Am. Chem. Soc. 126 (2004) 4566.
[35] P.J. Chmielewski, L. Latos-Grażyński, T. Głowiak, J. Am. Chem. Soc. 118 (1996) 5690.
[36] M. Stępień, L. Latos-Grażyński, J. Am. Chem. Soc. 124 (2002) 3838.
[37] M. Stępień, L. Latos-Grażyński, Chem. Eur. J. 7 (2001) 5113.
[38] E. Pacholska, L. Latos-Grażyński, Z. Ciunik, Angew. Chem. Int. Ed. 40 (2001) 4466.
[39] M. Toganoh, J. Konagawa, H. Furuta, Inorg. Chem. 45 (2006) 3852.
[40] T. Ishizuka, A. Osuka, H. Furuta, Angew. Chem. Int. Ed. 43 (2004) 5077.
[41] H. Furuta, T. Ishizuka, A. Osuka, T. Ogawa, J. Am. Chem. Soc. 122 (2000) 5748.
[42] A. Berlicka, L. Latos-Grażyński, T. Lis, Angew. Chem. Int. Ed. 44 (2005) 5288.
[43] A. Berlicka, N. Sprutta, L. Latos-Grażyński, Chem. Commun. (2006) 3346.
[44] A. Krivokapic, A.R. Cowley, H.L. Anderson, J. Org. Chem. 68 (2003) 1089.
[45] R. Myśliborski, L. Latos-Grażyński, L. Szterenberg, T. Lis, Angew. Chem. Int. Ed. 45 (2006) 3670.
[46] G.M. Badger, J.A. Elix, G.E. Lewis, Proc. Chem. Soc. (March) (1964) 82.
[47] Z. Hu, J.L. Atwood, M.P. Cava, J. Org. Chem. 59 (1994) 8071.
[48] N. Kobayashi, Y. Takeuchi, A. Matsuda, Angew. Chem. Int. Ed. 46 (2007) 758.
[49] C.-H. Lee, K.-T. Oh, Tetrahedron Lett. 40 (1999) 1921.
[50] E. Vogel, N. Jux, J. Dörr, T. Pelster, T. Berg, H.-S. Böhm, F. Behrens, J. Lex, D. Bremm, G. Hohlneicher, Angew. Chem. Int. Ed. 39 (2000) 1101.
[51] N. Jux, P. Koch, H. Schmickler, J. Lex, E. Vogel, Angew. Chem., Int. Ed. Engl. 29 (1990) 1385.
[52] J. Skonieczny, L. Latos-Grażyński, L. Szterenberg, Chem. Eur. J. 14 (2008) 4861.
[53] Y. Hirata, H. Furuta, A. Srinivasan, Nippon Kagakkai Koen Yokoshu 85 (2005) 1418.
[54] Z. Duan, M. Clochard, B. Donnadieu, F. Mathey, F.S. Tham, Organometallics 26 (2007) 3617.
[55] E. Vogel, M. Bröring, C. Erben, R. Demuth, J. Lex, M. Nendel, K.N. Houk, Angew. Chem., Int. Ed. Engl. 36 (1997) 353.
[56] E. Vogel, P. Scholz, R. Demuth, C. Erben, M. Bröring, H. Schmickler, J. Lex, G. Hohlneicher, D. Bremm, Y.-D. Wu, Angew. Chem. Int. Ed. 38 (1999) 2919.
[57] L. Latos-Grażyński, E. Pacholska, P.J. Chmielewski, M.M. Olmstead, A.L. Balch, Angew. Chem., Int. Ed. Engl. 34 (1995) 2252.
[58] C.D. Stevenson, T.L. Kurth, J. Am. Chem. Soc. 122 (2000) 722.
[59] J.F.M. Oth, H. Baumann, J.M. Gilles, G. Schröder, J. Am. Chem. Soc. 94 (1972) 3498.
[60] E. Pacholska-Dudziak, J. Skonieczny, M. Pawlicki, L. Szterenberg, Z. Ciunik, L. Latos-Grażyński, J. Am. Chem. Soc. 130 (2008) 6182.
[61] E. Heilbronner, Tetrahedron Lett. 29 (1964) 1923.
[62] D. Ajami, O. Oeckler, A. Simon, R. Herges, Nature 426 (2003) 819.
[63] D. Ajami, K. Hess, F. Köhler, C. Näther, O. Oeckler, A. Simon, C. Yamamoto, Y. Okamoto, R. Herges, Chem. Eur. J. 12 (2006) 5434.
[64] M. Stępień, L. Latos-Grażyński, N. Sprutta, P. Chwalisz, L. Szterenberg, Angew. Chem., Int. Ed. Engl. 46 (2007) 7869.
[65] J.K. Park, Z.S. Yoon, M.-C. Yoon, K.S. Kim, S. Mori, J.-Y. Shin, A. Osuka, D. Kim, J. Am. Chem. Soc. 130 (2008) 1824.
[66] Y. Tanaka, S. Saito, S. Mori, N. Aratani, H. Shinokubo, N. Shibata, Y. Higuchi, Z.S. Yoon, K.S. Kim, S.B. Noh, J.K. Park, D. Kim, A. Osuka, Angew. Chem. Int. Ed. 47 (2008) 681.
[67] E. Pacholska-Dudziak, J. Skonieczny, M. Pawlicki, L. Latos-Grażyński, L. Szterenberg, Inorg. Chem. 44 (2005) 8794.